Conversion of recoilless γ radiation into a periodic sequence of short intense pulses in a set of several sequentially placed resonant absorbers

Y. V. Radeonychev, V. A. Antonov, F. G. Vagizov, R. N. Shakhmuratov, and Olga Kocharovskaya

Conversion of recoilless γ radiation into a periodic sequence of short intense pulses in a set of several sequentially placed resonant absorbers

Y.V. Radeonychev[1,2,3,*], V.A. Antonov[1,2,3], F.G. Vagizov[3,5], R. N. Shakhmuratov[3,4]

and Olga Kocharovskaya[5]

[1] *Institute of Applied Physics, Russian Academy of Sciences,*
46 Ulyanov Street, Nizhny Novgorod, 603950, Russia,
[2] *N.I. Lobachevsky State University of Nizhny Novgorod,*
23 Gagarin Avenue, Nizhny Novgorod, 603950, Russia,
[3] *Kazan Federal University, 18 Kremlyovskaya Street,*
Kazan 420008, Republic of Tatarstan, Russia,
[4] *Kazan Physical-Technical Institute, Russian Academy of Sciences,*
10/7 Sibirsky Trakt, Kazan 420029 Russia
[5] *Department of Physics and Astronomy and*
Institute for Quantum Studies and Engineering,
Texas A&M University, College Station, TX 77843-4242, USA.

Abstract An efficient technique for producing a periodic sequence of short pulses of recoilless γ-radiation via its transmission through an optically thick vibrating resonant absorber was demonstrated recently [Nature, 508, 80 (2014)]. In this paper we extend the theoretical analysis to a case of multiple absorbers. We analyze a simple physical model describing control of spectral content of a frequency modulated γ-radiation by adjusting the amplitudes and initial phases of spectral components, using the resonant absorption and dispersion in a set of several sequentially placed resonant absorbers. On the basis of analytical solutions, we determine the ultimate possibilities of the proposed technique.

I. INTRODUCTION

In recent years, there has been an active search for methods of generating and controlling electromagnetic radiation with photon energy from several to tens of kiloelectronvolts (keV) [1-24]. This search is motivated by the potential to significantly extend existing diagnostic capabilities [1, 2, 5, 7-15], including high-precision spatial measurements [2, 5] and structural time-resolved studies of fast physical, chemical, and biological processes [7-15]. Shortening the wavelength enables one to reduce the diffraction-limited focus spot, which opens up novel possibilities in high-precision lithography [16] and focusing radiation to extremely large intensities [17]. Novel opportunities in quantum optics emerge in the X-ray domain [1, 6, 18]. One of the main directions of research in this area is to adapt the concepts of nonlinear and coherent optics to the keV photon energy range [1-4, 11, 18-24].

However, since the photon energies in this range are far above the ionization potential of atoms, the possibilities of utilizing these concepts in cases of interaction of 1-10 keV photons with bound electrons are rather limited. At the same time, photons of such energies can effectively interact with nuclei. Of particular importance here are the processes of recoilless resonant interactions of γ-photons with nuclei based on the Mössbauer effect [18, 25-47]. Several analogues of the well-known optical effects were observed in the resonant recoilless interaction of γ-photons with nuclei, such as ac-Stark splitting [31], the so-called gamma-echo effect [33-36], magnetic switching of nuclear forward scattering [38-40], the collective Lamb shift [41], cavity electromagnetically induced transparency [42], slowing down γ-photons in a doublet structure of the nuclear transition [29], single-photon revival in nuclear absorbing multilayer structures [43], and vacuum-assisted generation of coherences [44].

Most recently, an efficient converter of Mössbauer radiation of a radioactive source into a periodic sequence of short pulses was demonstrated [45]. The converter is constituted of a stainless steel foil with ^{57}Fe nuclei placed in the path of propagation of 14.4 keV recoilless

radiation emitted by a radioactive source, ^{57}Co (Fig. 1). The foil harmonically vibrates along the propagation direction of radiation. The spectral and temporal conversion of radiation occurs as a result of its resonant interaction with ^{57}Fe nuclei during the passage through the optically thick foil. Tuning the frequency and amplitude of vibration, resonance energies of the emitting nuclei in respect to the absorbing ones, and thickness of the foil enables control of the shape, duration and repetition period of the produced pulses. Pulses with a minimum duration of 18 ns were obtained in [45]. Such a technique is based on the quite general approach to control the spectral-temporal properties of radiation in various frequency ranges [48-58]. In the γ-ray domain, that approach for pulse shaping is successful owing to the following three basic factors. (i) Very short wavelengths of radiation (≈0.86Å for 14.4keV transition of ^{57}Co) and uniquely large ratios of the resonance nuclei energy to the linewidth (≈3×10^{12} for 14.4keV transition of both ^{57}Co and ^{57}Fe) make utilization of the Doppler effect in the photon-nuclei interaction effective for controlling the resonance energies of the source relative to the converter. (ii) Harmonic Doppler modulation of the resonance energy of the converter with respect to photon energy of the source via vibration enables one to generate a wide spectrum of radiation sidebands with predetermined initial phases. (iii) Resonant alteration of the selected spectral components of the photons inside the converter makes it possible to build the phase aligned spectrum corresponding to the pulsed waveforms of radiation.

In this paper, we further develop the above technique, extending it to the case of multiple resonant absorbers. We consider an analytical model describing the control of spectral content of a frequency-modulated γ-radiation by adjusting the amplitudes and initial phases of spectral components using the resonant absorption and dispersion in a set of several sequentially placed resonant absorbers. We discuss the possibilities of shortening the pulses and increasing their maximum peak intensity, as well as forming more complicated temporal waveforms.

The paper is organized as follows. Section II describes the theoretical model. In section III, we study analytically the techniques for building the phase-matched spectra corresponding to various temporal waveforms based on the deletion of a single or several components from the spectrum of the frequency-modulated radiation via their attenuation in a single or several sequentially placed resonant absorbers. In section IV, we analytically investigate the techniques for building the phase-aligned spectra corresponding to periodic sequences of pulses with higher peak intensity and shorter duration based on shifting of initial phases of the mismatched components of the spectrum of frequency-modulated radiation in properly tuned resonant absorbers. Section V is a summary of the results.

II. THE MODEL

Our study is based on the analytical solutions of the following model. The photons emitted by a radioactive source form a flow of γ-radiation. Taking into account the extreme narrowness of the recoilless spectral line of the source, we consider the emitted radiation as a monochromatic wave. As shown in [45] and below in this paper, this approximation gives good qualitative as well as quantitative agreement with the experimental results of [45] and the models, considering the Lorenzian shape of γ-radiation with definite linewidth [46, 47 and references therein]. Thus the electric field of radiation emitted in the direction to the absorbers, E_{em}, can be written as

$$E_{em}(\tau) = E_0 e^{-i\omega_0\tau}. \tag{1}$$

Here E_0 is the amplitude of the electric field, determined as $E_0 = \sqrt{8\pi I_0/c}$, where I_0 is the intensity of radiation experimentally found as $I_0 = N\hbar\omega_0/s$ (where $\hbar\omega_0$ is the energy of photon emitted by the source, and N is the average number of photons registered per unit time per unit square s), and $\tau = t - z/c$ is the local time in the reference frame co-moving with γ-ray photons along "z"-direction with the speed of light in vacuum c. The field (1) propagates through a

resonant absorber, which is a layer of a medium containing recoilless nuclei with quantum transition near-resonant to the field.

The photon energy, $\hbar\omega_0$, can be made harmonically modulated in respect to the energy of quantum transitions of the absorber nuclei by two ways. The first way is to fix the absorber and vibrate the source as a whole along the propagation direction of the field (1), such that coordinate z in the laboratory reference frame is related to the corresponding coordinate z_s in the reference frame associated with nuclei of the vibrating source, as

$$z = z_s - R\sin(\Omega t + \vartheta_0),\tag{2}$$

where R, Ω, and ϑ_0 are the amplitude, angular frequency, and initial phase of vibration, respectively. This relation is valid if thickness of the source, L_s, meets inequality $L_s \ll 2\pi V_{sound}^s/\Omega$, where V_{sound}^s is the speed of sound inside the source. The field (1) emitted by the vibrating source takes, because of the Doppler effect, the form of the frequency-modulated wave in the laboratory reference frame [27],

$$E_{em}(\vartheta_0, \tau) = E_0 e^{-i(\omega_0\tau - P\sin(\Omega\tau + \vartheta_0))}\tag{3}$$

where $P = R\omega_0/c$ is the modulation index.

The second way is to fix the source and vibrate the absorber along the propagation direction of the field (1), such that coordinate z in the laboratory reference frame is related to the corresponding coordinate z_a in the reference frame associated with nuclei of the moving absorber, as

$$z = z_a + R\sin(\Omega t + \vartheta_0).\tag{4}$$

Similarly, thickness of the absorber, L_A, should meet the relation $L_A \ll 2\pi V_{sound}^A/\Omega$, where V_{sound}^A is the speed of sound inside the absorber. Being monochromatic in the laboratory reference frame, field (1) takes the form (3) (where $\tau = t - z_a/c$) in the reference frame of the vibrating absorber.

The spectrum of the frequency-modulated field (3) consists of discrete components separated by the vibration frequency,

$$E_{em}(\vartheta_0, \tau) = E_0 e^{-i\omega_0\tau} \sum_{m=-\infty}^{\infty} J_m(P)e^{im(\Omega\tau + \vartheta_0)} = \sum_{n=-\infty}^{\infty} \tilde{E}_n e^{-i\omega_n\tau} = \sum_{n=-\infty}^{\infty} E_n(\vartheta_0, \tau)\tag{5}$$

where $\omega_n = \omega_0 + n\Omega$ and $\tilde{E}_n = E_0 J_{-n}(P)e^{-in\vartheta_0}$ are the frequency and complex amplitude of the nth spectral component, respectively, and $J_{-n}(P)$ is the Bessel function of the first kind meeting the relation $J_{-n} = e^{-i\pi n} J_n$. The amplitudes of spectral components are determined by the amplitude of vibration via the Bessel functions, $|J_n(P)|$. The initial phases of spectral components are either $0 - n\vartheta_0$ (let us call them in-phase components) if $J_{-n}(P) > 0$, or $\pi - n\vartheta_0$ (let us call them antiphase components) if $J_{-n}(P) < 0$.

Let us consider the possible techniques for converting the frequency-modulated field (described by the equations (3) and (5)) with time-independent amplitude E_0 into an amplitude-modulated field having a form of a periodic sequence of short γ-ray pulses with the peak height noticeably exceeding the amplitude E_0. It is known that a periodic sequence of pulses with minimum duration corresponds to the widest spectrum of equidistant, perfectly synchronized frequency components. In the best case, the phase difference between the neighboring spectral components is a constant value over the whole spectrum, i.e., the components are phase-aligned. The corresponding pulses, called bandwidth-limited pulses, have minimum possible durations, and the bursts between the pulses have the smallest height. If, in addition, all the frequency components have the same amplitude, the peak intensity of the pulses achieves the maximum limit, whereas the pedestal vanishes. The equidistant spectrum (5) of the frequency-modulated

field (3) can be very wide in the case of large values of the modulation index, P (the spectrum width is normally evaluated as $\Delta\omega=2(P+1)\Omega$). However, the amplitudes and initial phases of the spectral components have specific magnitudes such that superposition of the corresponding monochromatic waves results in the field having constant amplitude, $|E(\tau)|=E_0$. Therefore, in order to convert the field (3) into a pulse train, one needs to correct amplitudes and phases of the spectral components. As noted above, the nonresonant methods of nonlinear optics to align phases of the spectral components fail to be implemented in a keV domain because of strong attenuation of radiation due to photoionization [27]. Let us consider how the resonant properties of recoilless absorbing nuclei can be utilized to build a phase-aligned spectrum of Mössbauer radiation corresponding to a periodic sequence of pulses.

Let the field (3) propagate through one or several sequentially placed absorbers having spectral lines of the resonant transitions narrower than the frequency interval between the spectral components. Tuning the spectral lines of the absorbers to the frequencies of the chosen spectral components results in selective alteration of these components. In some cases, the neigboring spectral components can also be noticeably modified by the absorbers. As a result, the selective alteration of the complex amplitudes of N spectral components with numbers $m = \underbrace{a,b,c,...}_{N}$ of the spectrum (5) due to the resonant absorption and phase incursion can be described by the relation

$$E_{tr}(a,b,...,\vartheta_0,\tau) = E_{em}(\vartheta_0,\tau) \underbrace{-(1-\tilde{\eta}_a)\tilde{E}_a e^{-i\omega_a\tau} - (1-\tilde{\eta}_b)\tilde{E}_b e^{-i\omega_b\tau} - ...}_{N}, \tag{6}$$

where $E_{tr}(a,b,...,\vartheta_0,\tau)$ is the total transformed field after alteration of spectral components with numbers a, b, ... and the coefficient $\tilde{\eta}_m = e^{-\Lambda_m/2}e^{-i\Phi_m}$ (where $m=a,b,$ ...) describes the decrease of amplitude and incursion of phase of the mth spectral component. The selective modification of spectral components inside the resonant absorbers results in amplitude modulation of the transmitted field intensity, $I_{tr} = c|E_{tr}|^2/8\pi$. Below we discuss the cases where such a modulation constitutes periodic sequences of pulses.

III. DELETION OF SPECTRAL COMPONENTS

Let us consider deletion of a single or several spectral components via their selective attenuation in the properly tuned single or several resonant absorbers. If we assume that N components with numbers $m = \underbrace{a,b,c,...}_{N}$ are deleted from the spectrum (5), then we have $\tilde{\eta}_m = 0$ in (6) and the resulting field is

$$E_{del}(a,b,...,\vartheta_0,\tau) = E_{em}(\vartheta_0,\tau) \underbrace{-\tilde{E}_a e^{-i\omega_a\tau} - \tilde{E}_b e^{-i\omega_b\tau} - ...}_{N}. \tag{7}$$

Its intensity, $I_{del}=c|E_{del}|^2/8\pi$, registered by the detector behind the absorbers, can be written in the form:

$$I_{del}(a,b,...,\vartheta_0,\tau) = I_0 \left\{ 1 + \underbrace{J_{-a}^2 + J_{-b}^2 + ...}_{N} \right.$$

$$\underbrace{-2J_{-a}\cos(a\alpha + P\sin\alpha) - 2J_{-b}\cos(b\alpha + P\sin\alpha) - ...}_{N}$$

$$\left. \underbrace{+2J_{-a}J_{-b}\cos((a-b)\alpha) + 2J_{-a}J_{-c}\cos((a-c)\alpha) + 2J_{-c}J_{-b}\cos((c-b)\alpha) + ...}_{C_N^2} \right\} \tag{8}$$

where $I_0 = cE_0^2/8\pi$ is the intensity of radiation emitted by the source prior to any transformation, and $\alpha = \Omega\tau + \vartheta_0$.

Note that, according to (8), removing an arbitrary set of N components with numbers $\underbrace{a,b,c,...}_{N}$ from the spectrum (5) of the frequency-modulated field (3) results in the same temporal dependence of the intensity, as removing the set of N components with numbers $\underbrace{-a,-b,-c,...}_{N}$ (symmetrically located with respect to the carrier frequency ω_0) under the condition that initial phase ϑ_0 is shifted by π. In other words, the following relation is valid:

$$I_{del}(a,b,...,\vartheta_0,\tau) = I_{del}(-a,-b,...,\vartheta_0 \pm \pi,\tau). \tag{9}$$

The initial phase, ϑ_0, sets the time, τ_0, when the phase of vibration of the source or absorber equals zero. Its change results in shift of the temporal pattern of intensity as a whole in time. Below we assume that $\vartheta_0 = 0$.

As follows from (8), the intensity of the field passed through the absorbers, I_{del}, can periodically with period $T=2\pi/\Omega$ exceed the intensity of the field emitted by the source. The fist peak of the intensity is achieved at $\tau=0$,

$$I_{del}(a,b,...,\tau = 0) = I_0 \left(1 \underbrace{- J_{-a} - J_{-b} \cdots}_{N} \right)^2, \tag{10}$$

provided that $J_{-n}<0$ for $n=a,b,...$. This corresponds to the deletion of spectral components with initial phases of π (antiphase spectral components). The deletion of all antiphase components from the spectrum (5) would lead to formation of a train of bandwidth-limited pulses. The peak pulse intensity takes maximum value, $I_{del}(a,b,...,\tau = 0) = I_{del}^{max}(a,b,...)$, if the modulation index, P, provides maximum magnitude of the sum $\underbrace{|J_{-a}| + |J_{-b}| + ...}_{N}$. This can be explained as follows:

In order to provide the constant amplitude of the field (3), the antiphase spectral components compensate the in-phase components. Deletion of the antiphase components results in destruction of this balance. The larger total amplitude of the deleted components, the stronger disbalance takes place.

Let us study the conditions that cause the spectrally selective filtering of the field (3) in a single or several resonant absorbers to lead to pulse sequences with minimum pulse duration and maximum pulse height. If the modulation index $P<2.4$, the spectrum (5) consists of the central component at carrier frequency, ω_0, and no more than four significant sidebands of positive and four sidebands of negative orders, n, according to the magnitudes of the corresponding Bessel functions (Fig. 2). Two spectral components with indices $a=1$, $b=3$ are antiphase. In the case of $P=1.84$, realized in the proof-of-principle experiment [45], the amplitude of the third spectral component is small enough ($-J_{-3}(1.84)=0.1$, see Fig. 2, and Fig. 3 inset, black spectrum #1) and can be neglected. Then, according to (10), the maximum peak pulse intensity is achieved when the first component is deleted subject to $P=1.84$, namely $-J_{-1}(1.84) = 0.58 = \text{Max}$ corresponding to $I_{del}^{max}(1) = 2.5 I_0$ (Fig. 3, black line #1). At a larger modulation index, $P=2.3$, amplitude of the third spectral sideband is $-J_{-3}(2.3)=0.18$ while the sum $-J_{-3} - J_{-1}$ takes its maximum value, i.e., $-J_{-3}(2.3) - J_{-1}(2.3) = 0.72 = \text{Max}$. Therefore, removing both these spectral components (Fig. 3 inset, green spectrum #2) results in higher peak pulse intensity, $I_{del}^{max}(1;3) = 2.96 I_0$, and slightly shorter pulses (Fig. 3, green line #2). When modulation index $P>3$, three frequency components of the orders 0, 1, and 3 have significant amplitudes and are antiphase accordnig to the respective Bessel functions (Fig. 2). Their removal (Fig. 3 inset, blue spectrum #3) leads to formation of more intense and shorter pulses. The value $P=3.24$ maximizes the sum

$-J_{-3}(3.24) - J_{-1}(3.24) - J_0(3.24) = 0.93 = \text{Max}$ such that the maximum peak pulse intensity, according to (10), is $I_{del}^{max}(0;1;3) = 3.7I_0$ (Fig. 3, blue dashed line #3). Higher modulation indices allow formation of more intensive and shorter pulses via deletion of a large quantity of spectral components. However, this (i) reduces the average intensity of the pulses because of removal of more and more energy from the field, (ii) increases heights of bursts between the pulses because of non-equidistance of the resulting spectrum, and (iii) can increase the pedestal of the pulse sequence because of non-uniform distribution of energy over the spectrum.

Deletion of arbitrary spectral components at arbitrary modulation indices results in complicated temporal dependence of the intensity. According to (10), the temporal dependence of intensity is periodic with period of modulation of the field, $T=2\pi/\Omega$. Within the period, there are oscillations of intensity with various durations and amplitudes. This is the result of interference of the intensity oscillations at harmonics of vibration frequency, $\Omega_m=m\Omega$ ($m=a,b,...$), determined by the removed spectral components (the second group of N items in (8)), and oscillations at combination frequencies of these harmonics (the last group of C_N^2 items in (8)). The frequencies of harmonics, Ω_m, are modulated with vibration frequency Ω and modulation index P, such that they are time-dependent values, $\Omega_m(\tau) = \Omega_m + P\Omega\cos(\Omega\tau)$. At sufficiently large modulation indices, $P \geq m$, there are time intervals within the period T when $\Omega_m(\tau) \leq 0$. Such an uncommonly large frequency modulation of the intensity oscillations can lead to temporal dependence of intensity in the form of pulse sequence. Let us consider this regime in the simplest case where some a^{th} single spectral component is deleted at an arbitrary modulation index.

In this case, intensity (8) takes the form

$$I_{del}(a,\tau) = I_0\left\{1 + J_{-a}^2(P) - 2J_{-a}(P)\cos[a\Omega\tau + P\sin(\Omega\tau)]\right\}. \tag{11}$$

The instantaneous frequency of intensity oscillations, $\Omega_a(\tau) = a\Omega + P\Omega\cos(\Omega\tau)$, is the ath order harmonic of vibration frequency, $a\Omega$, sinusoidally modulated with modulation index P and vibration period $T = 2\pi/\Omega$. In the case where the modulation index is less than the order "a" of the removed spectral component, $P < a$, there are "a" oscillations of intensity within the period T. The intensity oscillations look like a monochromatic signal with single-tone frequency modulation. They have the same maxima $I_{del}^{max}(a) = I_0\left\{1 + |J_a(P)|\right\}^2$, and minima, $I_{del}^{min}(a) = I_0\left\{1 - |J_a(P)|\right\}^2$. They are the shortest and tightest at the beginning and at the end of period T, while they are elongated and more separated in time at the middle of period T. In the case where $P=a$, there are still "a" oscillations of intensity within the period T. However, the instantaneous frequency of oscillations, $\Omega_a(\tau)$, is equal to $2a\Omega$ at the beginning and at the end of period T and has a magnitude of zero at the middle of the period, $\Omega_a(\pi/\Omega) = 0$. At the middle of period T, the phase of intensity oscillations equals $a\pi$ (Fig. 4a, blue line #1), which ensures the lowest value of intensity, $I_{del}(a,\pi/\Omega) = I_0\left\{1 - |J_a(a)|\right\}^2$ and the largest temporal interval between the nearby crests of intensity. As a whole, such oscillations look like bunches of pulses (Fig. 4b, blue line #1). In cases where $P > a$, the instantaneous frequency of oscillations, $\Omega_a(\tau)$, is the sign-changing value. Therefore, there are three different times that the phase of intensity oscillations, $\Phi(\tau) = a\Omega\tau + P\sin(\Omega\tau)$, has the magnitude of $a\pi$ (Fig. 4a, red line #2). This means that a pair of new bursts (absent when $P \leq a$) appear in the middle of period T. If the modulation index slightly exceeds the number of the deleted component, $P = a + \xi$ (where $\xi << 1$), the heights of the new bursts is small ($I_{del}^{max} - I_{del}^{min} \approx 4I_0|J_a|a\xi$). However, these small bursts enlarge the time interval between bunches of the strong oscillations and make them shorter (Fig. 4b, red line #2). It should be noted that for an arbitrary number $a>0$, the Bessel

function $J_a(P)$ takes the first maximum at the modulation index just slightly exceeding its order (Fig. 2). This is the reason why deletion of the component with maximum amplitude from the field spectrum (3) leads to formation, within the vibration period, of a single (if $a=1$) or several (if $a>1$) pulses grouped into bunches with $N=a$ pulses in a bunch [45, 46]. Bunches are separated by a pair of relatively small bursts (Fig. 3 black line #1 and Fig. 4b red line #2). Increase of the modulation index leads to increase of amplitude of these bursts up to the amplitude of the bunched strong oscillations, $I_{del}^{max}(a)=I_0\left\{1+\left|J_a(P)\right|\right\}^2$, when the phase $\Phi(\tau)$ achieves the magnitude $(a+1)\pi$. Further increase of the modulation index leads to the appearance of the next pair of bursts. It also leads to the appearance of an intermediate group of strong oscillations of intensity due to the negative magnitudes of the instantaneous frequency, $\Omega_a(\tau)$, (Fig. 4a) and so on. Thus, in cases where $P \gg a$, there are large numbers of intensity oscillations within the period, T (Fig. 4, green lines #3). Their depth, $I_{del}^{max}-I_{del}^{min}=4I_0\left|J_a\right|$, is quite small because of a small value of the Bessel function, $\left|J_a(P)\right|\approx\sqrt{2/\pi P}$ and their quantity, N, inside the period, T, is determined by the modulation index, $N=\lfloor 2P/\pi \rfloor$ (where the brackets mean the floor function). If $P=\pi N/2+\xi$ (where $0<\xi\ll1$), then amplitude of the $(N+1)^{th}$ oscillation is small, $I_{del}^{max}-I_{del}^{min}\approx I_0\left|J_a\right|\xi^2$. As a result, the oscillations of intensity look like groups of pulses (Fig. 4, green lines #3).

Removal of the spectral components with indices $a,b,\ldots$ from the frequency-modulated γ–radiation (3), emitted by the vibrating source, may be implemented by arranging resonant recoilless absorbers "$A,B,\ldots$" sequentially along the z-axis with individually tuned z-projections of the constant velocities, $V_z(A)$, $V_z(B),\ldots$ (Fig. 5). The resonant frequency of the moving absorber "A" is shifted because of the Doppler effect, $\omega_A=\omega_{A0}\left(1-V_z(A)/c\right)$ (where ω_{A0} is the resonant frequency of the stationary absorber, and c is the speed of light). The proper magnitude of $V_z(A)$ provides coincidence of the absorber resonant frequency with frequency of the ath spectral component of the incident radiation (3). In this case, the field of the ath spectral component at the exit of the absorber has the form

$$E_a(\tau)=\tilde{E}_a e^{-i(\omega_a\tau+\Phi_a)}e^{-\Lambda_a/2}, \tag{12}$$

where

$$\Phi_a=\frac{T_A}{2}\frac{(\omega_a-\omega_A)/\gamma_A}{1+(\omega_a-\omega_A)^2/\gamma_A^2} \text{ and } \Lambda_a=T_A\frac{1}{1+(\omega_a-\omega_A)^2/\gamma_A^2} \tag{13}$$

are the phase incursion due to the resonant dispersion and the exponent of the intensity attenuation due to the resonant absorption at the frequency ω_a of the ath spectral component, respectively, $T_A=f_A\dfrac{4\pi\omega_A N_A\left|d_A\right|^2 L_A}{\gamma_A\hbar c}$ is the optical thickness of the absorber "A" at its transition frequency ω_A called Mössbauer thickness of the absorber, f_A is the Lamb-Mössbauer factor (the ratio of recoilless to total nuclear resonant absorption), N_A is the density of the resonant nuclei, d_A is the matrix element of the of dipole moment of the corresponding quantum transition, L_A is the thickness of the absorber, and γ_A is the halfwidth of the spectral line of the resonant transition. Let us assume that the frequency of the spectral line of the stationary source equals the frequency of the spectral line of the stationary absorber, $\omega_{A0}=\omega_0$. Then movement of the absorber with velocity $V_z(A)=-ac\Omega/\omega_0$ tunes the frequency of its spectral line to the frequency of the ath sideband of the field described by Eqs. (3),(5), $\omega_a-\omega_A=0$. In this case $\Phi_a=0$, $\Lambda_a=T_A$. Selective filtering the ath sideband occurs if the influence of the absorber on adjacent sidebands is negligible. This condition can be fulfilled if (i) the modulation frequency essentially

exceeds halfwidth of the spectral line of the absorber ($\Omega \gg \gamma_A$) and (ii) the following relations are valid:

$$\Lambda_{a\pm1} \cong T_A \left(\gamma_A / \Omega \right)^2 \ll 1, \ |\Phi_{a\pm1}| \cong T_A \gamma_A / \Omega \ll 1 . \tag{14}$$

Let us consider the conditions similar to the conditions experimentally realized in [45]. The radioactive source ^{57}Co of 14.4 keV photons vibrates with a frequency of $\Omega/2\pi=10$ MHz. This provides a modulation index of $P=1.84$. The resonant spectral line of the absorber has width of $2\gamma_A/2\pi=1$ MHz. The Mössbauer thickness of the absorber is $T_A=5$ which is realized in a stainless steel foil of thickness $L_A=25$ μm with natural abundance of nuclide ^{57}Fe (~2%) [45]. The frequency of the resonant spectral line of the absorber is tuned to the frequency of the first sideband of the emitted field, $\omega_A = \omega_0 + \Omega$, via its movement with a velocity of $V_z(A)=-0.96$mm/s. Then, according to (13), the intensity of the first sideband at the exit of the absorber is $I_1^{out}=I_1^{inp}e^{-\Lambda_1}=I_1^{inp}e^{-T_A}=0,007 I_1^{inp}$ (where I_1^{inp} is the intensity of the first sideband at the entrance into the absorber). For the nearest zeroth and the second spectral components, optical thickness of the absorber is $\Lambda_0=\Lambda_2\approx T_A \gamma_A^2 / \Omega^2=0.0125$, which provides the output intensities $I_0^{out}/I_0^{inp}=I_2^{out}/I_2^{inp}=0.99$ and the phase shifts $|\Phi_0|=|\Phi_2|\approx T_A \gamma_A / \Omega=0.08\pi$. Thus, deletion of the first spectral component of the frequency-modulated γ-radiation by a recoilless resonant absorber under the above conditions is selective with high accuracy. Such a deletion leads to formation of a sequence of pulses plotted in Fig. 3 (black line #1) which are similar to pulses in [45]. Use of one more stainless steel foil "B" with the same as "A" parameters, moving with a velocity of $V_z(B)=-2.88$mm/s, would provide the selective deletion of the third spectral sideband. At the modulation index of $P=2.3$, this would lead to an increase of the peak pulse intensity as discussed above (Fig. 3 green line #2). Similarly, three stainless steel foils with velocities $V_z(A)=0$, $V_z(B)=-0.96$mm/s, and $V_z(C)=-2.88$mm/s at the modulation index of $P=3.24$ selectively delete three spectral components (Fig. 5), further increasing the peak pulse intensity and shortening the pulse duration similar to Fig. 3 blue dashed line #3.

The propagation of γ-radiation through the absorbers is accompanied by the non-resonant attenuation of radiation as a whole owing to photoelectric effect. Taking into account the photoelectric absorption, the intensity of the field behind the absorbers can be written as

$$I_{tr}^{pha} = I_{tr} e^{-\mu_A L_A - \mu_B L_B - \dots} , \tag{15}$$

where I_{tr} is the intensity of the transformed field, (6), while μ_Z and L_Z ($Z=A,B,\dots$) are, respectively, the linear photoelectric absorption coefficient and the thickness of the corresponding absorber. The reduction of intensity in an absorber due to photoelectric absorption for a given magnitude of the Mössbauer thickness, T_A, is ultimately determined by the percentage of the resonant nuclei: the higher the percentage of the resonant nuclei, the smaller thickness, L_A, of the absorber and, hence, the smaller photoelectric attenuation. The minimum photoelectric attenuation of intensity occurs in the case where all atoms of an absorber contain the resonant nuclei. For example, in the ideal case of an absorber consisting of atoms with ^{57}Fe nuclei only, the linear photoelectric absorption coefficient is $\mu=4.95\times10^4 m^{-1}$ [59]. This means that the Mössbauer thickness of $T_A=5$ corresponds to $L_A=0.35\mu m$, leading to very weak photoelectric attenuation of intensity in the absorber, $I_{del}^{pha} = I_{del}e^{-0.018} = 0.98 I_{del}$ (where I_{del}^{pha} is the intensity of the transformed radiation obtained via deletion of a single spectral component, taking into account the photoelectric absorption). However, in the case of stainless steel foil of the chemical compound Fe:Cr:Ni at 70:19:11 wt% (Type 304), and natural abundance of nuclide ^{57}Fe (~2%), the Mössbauer thickness of $T_A=5$ corresponds to the foil thickness of $L_A=25$ μm. The linear photoelectric absorption coefficient in this case is $\mu=5.06\div5.17\times10^4 m^{-1}$ [59]. As a result, one has

strong photoelectric attenuation of intensity in the absorber up to the value $I_{del}^{pha} = I_{del}e^{-1.3} = 0.27I_{del}$.

There is an option to selectively delete two spectral components of frequency-modulated γ-radiation emitted by a vibrating source by means of a single resonant absorber with a split spectral line. This option can be implemented at the specific magnitude of vibration frequency equal to the frequency splitting of the absorber spectral line. For example, the absorber $FeC_2O_4 \cdot 2H_2O$ has the spectral line, split at ≈17.9 MHz [29]. It could be used for simultaneous selective deletion of the first and third sidebands subject to the vibration frequency of 8.95 MHz, or for the deletion of the adjacent zero and first sidebands subject to the vibration frequency of 17.9 MHz. Similarly, one can use the absorber $FeTiO_3$ with split at 6.98 MHz spectral line or the absorber $Fe_2(SO_4)_3 \cdot xH_2O$ with split at 5.6 MHz spectral line [29].

In the case where the pulse sequence is formed in a vibrating absorber, (4), from radiation emitted by a stationary source, all the above discussions and formulae (7)-(14) are valid if they are referred to the reference frame, comoving with the absorber. After coming back to the laboratory reference frame, the field passed across the vibrating absorber has a form differing from (7) by the factor $e^{-iP\sin(\Omega\tau+\vartheta_0)}$,

$$E_{del}^{lab}(a,b,...,\vartheta_0,\tau) = e^{-iP\sin(\Omega\tau+\vartheta_0)} \sum_{n=-\infty}^{\infty} \tilde{E}_n e^{-i\omega_n\tau} \underbrace{-\tilde{E}_a e^{-i\omega_a\tau} - \tilde{E}_b e^{-i\omega_b\tau} - ...}_{N}, \qquad (16)$$

whereas the intensity keeps the form (8). The transformation of recoilless γ–radiation into the pulse sequence in a single vibrating absorber has been realized in [45]. In that case, tuning the spectral line of an absorber to the definite sideband of radiation was realized via moving the source with a constant velocity along the z-direction. In order to use several vibrating absorbers for the selective deletion of several spectral components, one should provide synchronization of vibrations of all the absorbers with the same frequency and their movement with individual constant velocities along the z-direction.

IV. PHASE INVERSION OF SPECTRAL COMPONENTS

As noted in section II, the spectrum (5) of the frequency-modulated radiation, (3), consists of in-phase and antiphase components with initial phases of $0 - n\vartheta_0$ and $\pi - n\vartheta_0$, respectively. Therefore, the selective inversion (i.e., shift by π) of the initial phases of either antiphase or in-phase components using the resonant dispersion of the properly tuned absorbers would result in the phase-aligned spectrum corresponding to a periodic sequence of bandwidth-limited pulses. Their peak intensity would be essentially higher, the pedestal and bursts between the pulses would be essentially smaller compared to the case of deletion of the mismatched spectral components, since the energy is not removed from the field and the spectrum remains equidistant.

Inversion of initial phases of N arbitrary spectral components of the spectrum (5) with numbers $m = \underbrace{a,b,c,...}_{N}$ corresponds to $\tilde{\eta}_m = -\eta_m$, where $\eta_m = e^{-\Lambda_m/2}$ in (6). The resulting field,

E_{inv}, and its intensity, $I_{inv}=c|E_{inv}|^2/8\pi$, are, respectively,

$$E_{inv}(a,b,...,\vartheta_0,\tau) = \sum_{n=-\infty}^{\infty} \tilde{E}_n e^{-i\omega_n\tau} \underbrace{-(1+\eta_a)\tilde{E}_a e^{-i\omega_a\tau} - (1+\eta_b)\tilde{E}_b e^{-i\omega_b\tau} - ...}_{N}, \qquad (17)$$

and

$$I_{inv}(a,b,...,\vartheta_0,\tau) = I_0 \left\{ 1 + \underbrace{G_{-a}^2 + G_{-b}^2 + ...}_{N} \right.$$

$$\underbrace{-2G_{-a}\cos(P\sin\alpha + a\alpha) - 2G_{-b}\cos(P\sin\alpha + b\alpha) - ...}_{N}$$

(18)

$$\left. \underbrace{+2G_{-a}G_{-b}\cos((a-b)\alpha) + 2G_{-a}G_{-c}\cos((a-c)\alpha) + 2G_{-c}G_{-b}\cos((c-b)\alpha) + ...}_{C_N^2} \right\}$$

where $G_m = (1+\eta_m)J_m$. According to (18), inversion of initial phases of N arbitrary components with numbers $\underbrace{a,b,c,...}_{N}$ of the spectrum (5) of the frequency-modulated field (3) results in the same temporal dependence of the intensity as in the case of inversion of initial phases of N components with numbers $\underbrace{-a,-b,-c,...}_{N}$ (symmetrically located with respect to the carrier frequency ω_0) under the condition where the initial phase ϑ_0 is shifted by π. In other words, the following relation is valid:

$$I_{inv}(a,b,...,\vartheta_0,\tau) = I_{inv}(-a,-b,...,\vartheta_0 \pm \pi,\tau). \tag{19}$$

Therefore, similar to the previous paragraph, we assume below that $\vartheta_0 = 0$ and consider inversion of initial phases of antiphase components only.

Comparison of formulae (7)-(9) with formulae (17)-(19) shows that the selective phase inversion is formally similar to deletion of the spectral components. Similar to (10), the highest peak pulse intensity is achieved at $\tau=0$ and equals

$$I_{Inv}(a,b,...,\tau=0) = I_0 \left(1 \underbrace{- G_{-a} - G_{-b}...}_{N} \right)^2. \tag{20}$$

The peak pulse intensity takes its maximum value, $I_{inv}(a,b,...,\tau=0) = \max\{I_{inv}(a,b,...)\}$, when all the antiphase spectral components with noticeable amplitudes are inverted and the vibration amplitude provides the optimal value of modulation index, P, such that sum $-G_{-a} - G_{-b}...$ takes the largest magnitude. As follows from (10) and (20), inversion of initial phases of antiphase components allows one to increase the maximum peak pulse intensity less than four times, $\max\{I_{inv}(a,b,...)\} / \max\{I_{del}(a,b,...)\} < 4$, compared to the case of deletion of these components at the same parameter magnitudes and under the ideal conditions where the only change in the spectrum (5) is either phase inversion or deletion of the components. As discussed below, this ratio is usually reduced depending on the possible implementations and yet unaccounted for factors.

The resonant dispersion is inevitably accompanied by the resonant absorption. Therefore the optimal conditions for the selective resonant inversion of the initial phase of the ath spectral component should imply a proper detuning of the absorber resonant frequency from the frequency of the ath component, $\delta_a = \omega_a - \omega_A$, in order to minimize attenuation of this component and to minimally alter the adjacent components. If $\delta_a > 0$, then it follows from (13) that larger detuning leads to weaker resonant absorption of the ath spectral component but stronger influence of the absorber resonant transition on the nearest $(a-1)^{th}$ component. For example, if the vibration frequency is $\Omega = 20\gamma_A$ (corresponding to $\Omega/2\pi=10$ MHz in the experiment with ^{57}Fe, [45]) and the detuning is $\delta_a = 3\gamma_A$, then, according to (13), inversion of the initial phase of the ath spectral component occurs at Mössbauer thickness $T_A=20.9$. This leads to both strong resonant

attenuation of this component (its intensity at the exit of the absorber is $I_a^{out}=0,12I_a^{inp}$, Fig. 6a) and noticeable change of the $(a-1)^{th}$ component (the phase incursion is $\Phi_{n-1}=-0.2\pi$ and the output intensity is $I_{a-1}^{out}=0,93I_{a-1}^{inp}$). This means that inversion of the initial phase of the first spectral component in one resonant absorber or both the first and third components in two resonant absorbers, under the conditions discussed in Sec. III, has no significant advantage over the selective resonant deletion of these components. Moreover, the large Mössbauer thickness of the absorber ($T_A=20.9$) means noticeable reduction of intensity as a whole due to photoelectric absorption, especially if two absorbers are used. However, in cases where $\Omega>>\delta_a>>\gamma_A$, the resonant dispersion can provide selective inversion of the initial phase of the ath component since, according to (13), one has $\Lambda_a\approx2\pi\gamma_A/\delta_a<<1$, $\Lambda_{a-1}\approx\Lambda_a(\delta_a/\Omega)^2<<1$, and $|\Phi_{a-1}|\approx|-\pi\delta_a/\Omega|<<1$, subject to sufficiently large Mössbauer thickness of absorber, $T_A\approx2\pi\delta_a/\gamma_A>>1$. For instance, if $\Omega=100\gamma_A$ (corresponding to $\Omega/2\pi=50$ MHz in the case of ^{57}Fe, [45]) and $\delta_a=15\gamma_A$, one has $\Lambda_a=0.4$, $\Lambda_{a-1}=0,009$, $|\Phi_{a-1}|=0.15\pi$, and $T_A=94.3$, which correspond to rather weak resonant attenuation of the phase inverted a^{th} component ($I_a^{out}=0.67I_a^{inp}$) and small resonant alteration of the adjacent components. However, even in the case of the ideal absorber consisting of only atoms with ^{57}Fe nuclei, this requires the absorber thickness $L_A=6.6\mu m$ resulting, according to (15), in about 30% reduction of radiation intensity due to photoelectric absorption.

Utilization of the resonant dispersion can be useful when the modulation index, P, is such that two adjacent spectral components are antiphase. Such a situation occurs when $P>2.4$. In this case, the resonant spectral line of a single absorber can be tuned in the middle between these components (Fig. 6b). If the Mössbauer thickness of the absorber is $T_A=\frac{4\pi\gamma_A}{\Omega}\left(1+(\Omega/2\gamma_A)^2\right)$, then, according to (13), at the exit of the absorber the initial phase of the ath spectral component is shifted by π while the initial phase of the $(a-1)^{th}$ spectral component is shifted by $-\pi$. Thus, a resonant absorber with an unsplit spectral line simultaneously inverts initial phases of two spectral components. The resonant attenuation of both components is the same: $\Lambda_{a-1}=\Lambda_a=4\pi\gamma_A/\Omega$. The alteration of other spectral components, when $\Omega>>\gamma_A$, is defined by the relations: $\Lambda_{a-1-m}=\Lambda_{a+m}\approx\Lambda_a/(2m+1)^2$, $|\Phi_{a-1-m}|=|\Phi_{a+m}|\approx\pi/(2m+1)$, $m=1,2,...$ Thus, simultaneous inversion of initial phases of two spectral components in a single absorber instead of their deletion by two absorbers enables one (i) to transform the same spectrum with fewer resonant absorbers and (ii) to save two spectral components in the spectrum. The latter reduces both the pedestal of the pulse sequence and heights of bursts between the pulses, as well as increases the peak pulse intensity. However, (i) the components nearest to the phase-inverted ones acquire rather large phase shifts of $\pm\pi/3$ for $m=\pm1$, and $\pm\pi/5$ for $m=\pm2$ at the exit of the absorber, leading to lengthening of the pulses, and (ii) the required Mössbauer thickness of the absorber is quite large (the minimum value of T_A is $T_A^{min}=8\pi\approx25$, realized at $\Omega=2\gamma_A$, while in the case $\Omega>>\gamma_A$, one has $T_A\approx\pi\Omega/\gamma_A>>1$), which reduces the output intensity because of the photoelectric absorption.

For example, when vibration frequency is $\Omega=20\gamma_A$ and modulation index is $P=3.24$ (Fig. 3, blue dashed line and spectrum in inset #3), one can use a single absorber with Mössbauer thickness $T_A=63.5$ to invert initial phases of two spectral components #0 and #1 instead of using two absorbers with $T_A=5$ for their deletion (Fig. 7a). The exponent of the accompanied resonant absorption is $\Lambda_0=\Lambda_1=0.63$, corresponding to the output intensity of these components $I_0^{out}/I_0^{inp}=I_1^{out}/I_1^{inp}=0.53$. The nearest minus first and second components acquire the phase shift

of $\pm\pi/3$ and are resonantly attenuated such that $I_{-1}^{out}/I_{-1}^{inp}=I_2^{out}/I_2^{inp}=0.93$. Amplitude and phase alteration of the minus first and second components in addition to initial phase inversion of #0 and #1 and deletion of #3 components leads to modification of relations (10) and (20) such that the highest peak pulse intensity is achieved at optimal modulation index P=3.4 that was found numerically. The required Mössbauer thickness, T_A=63.5, in the case of an ideal ^{57}Fe absorber corresponds to the absorber thickness L_A=4.4μm leading, according to (15), to 20% reduction of intensity as a whole, $I_{inv}^{pha}=I_{inv}e^{-0.2}=0.8I_{inv}$ (where I_{inv}^{pha} and I_{inv} is the intensity of radiation after inversion of initial phases of two spectral components with and without photoelectric absorption, respectively) versus 4% reduction of intensity in two absorbers deleting these components. As a result, in the case of optimal modulation index P=3.4, use of the ideal absorber "A" with thickness L_A=4.4μm inverting initial phases of zero and the first spectral components, and sequentially placed absorber "B" with thickness L_B=0.35μm deleting the third component (Fig. 7a) leads to pulses with less peak intensity than that of pulses produced via deletion of all three components at optimal modulation index P=3.24 (Fig. 7b). However, the pedestal of the pulse sequence produced via phase inversion of the anti-phase spectral components is lower than the pedestal of the pulse sequence produced via deletion of these components, owing to more uniform distribution of energy over the spectrum in the former case. At higher magnitudes of the modulation index, P, optimal for pulse formation via deletion or inversion of the antiphase components, these differences also take place. If the ideal absorbers are replaced with compounds (like stainless steel foils), the difference in peak pulse intensity and pedestal becomes larger since the foil thicknesses and hence photoelectric absorption become larger with decreasing percentages of ^{57}Fe in compounds. Thus, in the case of a ^{57}Co source of γ-radiation and ^{57}Fe absorbing nuclei, use of N (N≥3) resonant absorbers for deleting the set of N antiphase spectral components from the spectrum of frequency-modulated radiation results in a periodic sequence of pulses with the same duration but larger peak intensity, pedestal, and bursts between the pulses as compared with use of $N-1$ resonant absorbers, one of which inverts phases of two spectral components of this set.

However, use of N (N≥3) resonant absorbers, one of which inverts initial phases of two adjacent spectral components, enables one to transform N+1 antiphase spectral components of the frequency-modulated radiation at higher modulation indices as compared with use of N resonant absorbers only deleting the spectral components. This can result in shorter pulses with higher peak intensity. For example, in the case where vibration frequency is Ω=20γ_A and the optimal modulation index is P=4.7, four spectral components are antiphase (Fig. 8a). In this case, three resonant absorbers are sufficient for their alteration: the absorber "A" with Mössbauer thickness T_A=63.5 inverts the components #−1 and #0, while the absorbers "B" and "C" with Mössbauer thickness T_B=T_C=5 delete the spectral components #3 and #5. This results in shorter pulses with higher peak intensity, using both ideal and stainless steel absorbers, as compared to the case of the same quantity of resonant absorbers with Mössbauer thickness T_A=5 deleting three spectral components at the optimal modulation index P=3.24 (Fig. 8b). The peak intensity of the produced pulses is more than four times higher than intensity of γ-radiation from the source, while the pulse duration is less than one tenth of the repetition period.

At larger magnitudes of the modulation index, several pairs of adjacent antiphase spectral components can occur. As seen from Fig. 2, pairs of spectral components of the following orders are antiphase: {-1,-2} and {2,3} for P≈6 since J_1,J_2 and J_{-2},J_{-3} are negative, {-2,-3} and {1,2} for P≈7.3 since J_2,J_3 and J_{-1},J_{-2} are negative, {-4,-3}, {1,2}, and {4,5} for P≈8 since J_3,J_4, J_{-1},J_{-2}, and J_{-4},J_{-5} are negative. Each pair can be phase-inverted by one respective absorber. Thus, use of the resonant dispersion allows one to obtain the widest spectrum of nearly phase-aligned equidistant components corresponding to the shortest pulses with minimum quantity of absorbers. For example, in the case of P≈8, the pulse duration of about T/20 (where the pulse repletion period

$T=2\pi/\Omega$ coincides with the vibration period) can be produced with 5 absorbers modifying 8 of 21 spectral components (three dispersive absorbers invert initial phases of 6 components). At $\Omega/2\pi=20$ MHz it corresponds to 2.5 ns pulses. However, the photoelectric absorption essentially reduces the intensity of γ-radiation as a whole in three dispersive absorbers. This reduction is much stronger than the reduction of intensity in 6 resonant absorbers selectively deleting the same components. As a result, the peak pulse intensity does not exceed $2.5I_0$. Thus, deletion of the antiphase spectral components in a set of multiple resonant absorbers is preferable for formation of short γ-ray pulses with high peak intensity.

In practice, production of a maximum number of phase-aligned spectral components corresponding to pulses with maximum peak intensity and minimum ratio of the pulse duration to the pulse repetition period is limited by the difficulty in providing sinusoidal vibration of an emitter or absorbers with required amplitude as well as by the difficulty in arranging a large number of resonant absorbers that move with individually tuned velocities. For example, formation of pulses with durations of 1/50 of the repetition period requires generation of about 50 spectral components; this can be achieved by a modulation index of about 20. In this case, 22 of 50 spectral components are antiphase and hence 22 resonant absorbers are needed to delete them. The peak intensity of the produced pulses is about an order of magnitude higher than intensity of radiation before the conversion. For the case of 14.4 keV radiation converted in the foils of ^{57}Fe, these estimations correspond to formation of ~1 ns pulses in 22 foils if the source vibrates with frequency of $\Omega/2\pi=20$ MHz and amplitude of $R=2.8$Å (Fig. 9). Much shorter pulses (without change of the ratio between the pulse duration and the pulse repetition period) can be obtained via increase of the vibration frequency. Vibration with the same amplitude but with frequency of 2 GHz [60, 61] would result in pulse duration of about 10 ps.

V CONCLUSION

In this paper, we studied the possible ways to develop the technique [45] of shaping recoilless γ-radiation of a radioactive source into a periodic sequence of short pulses via frequency modulation of radiation and transformation of its spectrum in resonant absorbing media. The possibilities of producing shorter γ-ray pulses with higher peak intensities were investigated. Our study was based on an analytical model that assumes γ-radiation to be a monochromatic wave with sinusoidally modulated carrier frequency. The frequency modulation of γ-radiation is provided by mechanical sinusoidal vibration of either a source or absorbing medium along the direction of radiation propagation. The resonant absorbing medium is used to transform the specific spectrum (consisting of in-phase and antiphase components) of the frequency-modulated radiation with time-independent intensity into a spectrum of phase-aligned components corresponding to a periodic sequence of pulses. Shortening of pulses and increase of their peak intensity is achieved via increase of the modulation index, which leads to appearance of more and more in-phase and antiphase components. We proposed to correct the phase mismatching between the spectral components and build the phase-aligned spectrum by using a set of several sequentially placed resonant absorbers. Two basic techniques were discussed.

The first technique is based on the selective deletion of all non-vanishing mismatched spectral components via their resonant absorption in the spectrally tuned absorbers such that the remaining components form the phase-aligned spectrum. The resulting pulses are nearly bandwidth limited. However, the pulse sequence can have a noticeable pedestal and rather intensive bursts between the pulses since the spectrum becomes non-equidistant after deletion of the spectral components. This technique can be realized with the modest Mössbauer thickness of the absorbers and therefore provides weak nonresonant attenuation of radiation as a whole due to photoelectric absorption. As a result, the peak pulse intensity can essentially exceed the intensity of radiation emitted by the source in the direction of the absorbers. The required quantity of the absorbers equals the quantity of the deleted spectral components. This factor can impede

shortening of the pulses because of the technical problems of managing a large number of absorbers. The deletion of more and more spectral components increases non-equidistance of the spectrum and reduces the average intensity of the pulses.

We also studied the selective deletion of arbitrary single spectral components from the spectrum of the frequency-modulated γ-radiation. We showed that there exist the optimal conditions when deleting a single spectral component of arbitrary order, m, to result in a periodic sequence of pulse bunches containing m pulses in a bunch.

Another technique is based on selective inversion of initial phases of the mismatched spectral components using the resonant dispersion of absorbers. This technique enables building of the equidistant spectrum of nearly aligned components. If the resonant frequency of an absorber is tuned in the middle between two adjacent spectral components, a single absorber can simultaneously phase-invert them both, reducing the number of absorbers required to build a wide, nearly phase-aligned spectrum. Hence, it potentially enables one to produce shorter pulses with fewer absorbers than the technique based on deletion of the components. The pulse sequence has a lower pedestal and smaller intermediate bursts. However, this technique needs substantially larger Mössbauer thicknesses of the absorbers, resulting in essential attenuation of radiation as a whole due to photoelectric absorption. As a result, shortening of pulses with larger numbers of the absorbers is accompanied by essential reduction of their peak intensity.

We considered the case of a ^{57}Co source of γ-radiation vibrating with a frequency of 10 MHz and various experimentally achievable amplitudes as well as various numbers of absorbers from one to three with different percentages of ^{57}Fe resonant nuclei. It was shown that taking into account the advantages of the discussed techniques and combining the dispersive and absorptive properties of the resonant absorbers, one can control peak pulse intensity, pulse duration, and pedestal of the pulse sequence. Use of three resonant absorbers in experimentally realizable conditions allows one to produce pulses with durations of about 8% of the vibration period and peak intensity of more than 4 times the primary radiation. We evaluated the ultimate possibilities of the proposed technique and showed that formation of periodic trains of picosecond γ-ray pulses from a ^{57}Co source could be realized. The basic limitations of the technique are the difficulty in providing sinusoidal vibration of an emitter or absorbers with required frequency and amplitude as well the difficulty of arranging a large number of resonant absorbers moving with individually tuned velocities.

IV. ACKNOWLEDGEMENTS

*Corresponding author: radion@appl.sci-nnov.ru

1. Ed. B. Adams, Nonlinear Optics, Quantum Optics, and Ultrafast Phenomena with X-rays, Kluwer Academic Publishers (2003).
2. Yu. V. Shvyd'ko, X-Ray Optics: High Energy-Resolution Applications, Springer Verlag (2004).

3. J. Amann et al., Demonstration of self-seeding in a hard-X-ray free-electron laser, Nature Photonics **6**, 693 (2012).
4. T. Popmintchev et al., Bright Coherent Ultrahigh Harmonics in the keV X-Ray Regime from Mid-Infrared Femtosecond Lasers, Science **336**, 12878 (2012).
5. G. Hajdok, J.J Battista, I.A. Cunningham, Fundamental x-ray interaction limits in diagnostic imaging detectors: spatial resolution, Med Phys. **35** 3180 (2008).
6. B.W. Adams, C. Buth, S. M. Cavaletto, J. Evers, Z. Harman, C. H. Keitel, A. Pálffy, A. Picón, R. Röhlsberger, Yu. Rostovtsev & K. Tamasaku, X-ray Quantum Optics, Journal of modern optics **60**, 2 (2013).
7. Rose-Petruck C., Jimenez R., Guo T., et al., Picosecond-milliangstrom lattice dynamics measured by ultrafast X-ray diffraction, Nature **398**, 310 (1999).
8. A.M. Lindenberg, I. Kagn, S.L. Jonson, et al., Time-resolved x-ray diffraction from coherent phonons during a laser-induced phase transition, Phys. Rev. Lett. **84**, 111 (2000).
9. D.A. Reis, M.F. DeCamp, P.H. Bucksbaum, et al., Probing impulsive strain propagation with X-ray pulses, Phys. Rev. Lett. **86**, 3072 (2001).
10. Eric A. Galburt, and Barry L. Stoddard, Time-resolved macromolecular crystallography, Physics Today **54**, No.7, 33 (2001).
11. M. Uesaka, H. Kotaki, K. Nakajima, et al., Generation and application of femtosecond X-ray pulse, Nuclear Instruments & Methods in Physics Research, Section A **455**, 90 (2000).
12. Barty, A. et al. Ultrafast single-shot diffraction imaging of nanoscale dynamics. Nature Photon. **2**, 415 (2008).
13. Bressler, C. et al. Femtosecond XANES study of the light-induced spin crossover dynamics in an iron(II) complex. Science **323**, 489 (2009).
14. M. Altarelli, A. P. Mancuso, Structural biology at the European X-ray free-electron laser facility, Phil. Trans. R. Soc. B, **369** 20130311 (2014).
15. R Neutze, Opportunities and challenges for time-resolved studies of protein structural dynamics at X-ray free-electron laser, Phil. Trans. R. Soc. B, **369** 20130318 (2014).
16. H. J. Levinson, Principles of Lithography, Second Edition, SPIE Press, Bellingham, WA (2005).
17. H. Yumoto et.al. Focusing of X-ray free electron laser pulses with reflective optics, Nature Photonics **7**, 43 (2013).
18. K. P. Heeg and J. Evers, X-ray quantum optics with Mössbauer nuclei embedded in thin-film cavities, Phys. Rev. A **88**, 043828 (2013).
19. S. Shwartz, et al. X-ray parametric down-conversion in the Langevin regime. Phys. Rev. Lett. **109**, 013602 (2012).
20. S. Shwartz, et al., X-Ray Second Harmonic Generation, Phys. Rev. Lett. **112**, 163901 (2014).
21. R. Röhlsberger, and J. Evers, Vacuum-Assisted Generation and Control of Atomic Coherences at X-Ray Energies Phys. Rev. Lett. **111**, 073601 (2013).
22. X. Zhang, A.A. Svidzinsky, Superradiant control of γ-ray propagation by vibrating nuclear arrays, Phys Rev. A **88**, 033854 (2013).
23. W.-T. Liao, A. Palffy, Proposed Entanglement of X-ray Nuclear Polaritons as a Potential Method for Probing Matter at the Subatomic Scale, Phys. Rev. Lett. **112**, 057401 (2014).
24. W.-T. Liao, A. Pálffy, C.H. Keitel, Coherent Storage and Phase Modulation of Single Hard-X-Ray Photons Using Nuclear Excitons, Phys. Rev. Lett. **109**, 197403 (2012).
25. P. Gütlich, E. Bill, A.X. Trautwein, Mössbauer Spectroscopy and Transition Metal Chemistry, Springer Verlag (2010).
26. Y. Rostovtsev, and O. Kocharovskaya, Modification of Mössbauer Spectra under the Action of Electromagnetic Fields, Hyperfine Interactions, **135**, 233 (2001).
27. E. Kuznetsova, R. Kolesov, and O. Kocharovskaya, Compression of gamma-ray photons into ultrashort pulses, Phys. Rev. A **68**, 043825 (2003).
28. G.V. Smirnov, General properties of nuclear resonant scattering, Hyperfine Interactions **123/124**, 31 (1999).

29. R. N. Shakhmuratov, F. Vagizov, J. Odeurs, and O. Kocharovskaya, Slow γ photon with a doublet structure: Time delay via a transition from destructive to constructive interference of collectively scattered radiation with the incoming photon, Phys. Rev. A **80**, 063805 (2009).

30. U. van Burck, Coherent pulse propagation through resonant media, Hyperfine Interactions **123/124**, 483 (1999).

31. F. Vagizov, The splitting of hyperfine lines of ^{57}Fe nuclei in RF magnetic field, Hyperfine Interactions **61**, 1359 (1990).

32. F.G. Vagizov, R.A. Manapov, E.K. Sadykov, L.L. Zakirov, The effect of radiofrequency modulation of Fe-57 hyperfine interaction by rotating magnetic field, Hyperfine Interactions, **116**, 91 (1998).

33. P. Helisto, I. Tittonen, M. Lippmaa, and T. Katila, Gamma echo, Phys. Rev. Lett. **66**, 2037 (1991).

34. I. Tittonen, M. Lippmaa, P. Helisto, and T. Katila, Stepwise phase modulation of recoilless gamma radiation in a coincidence experiment: Gamma echo, Phys. Rev. B **47**, 7840 (1993).

35. E. Ikonen, P. Helistö, T. Katila, and K. Riski, Coherent transient effects due to phase modulation of recoilless γ radiation, Phys. Rev. A. **32**, 2298 (1985).

36. P. Helistö, E. Ikonen, T. Katila, W. Potzel, and K. Riski, Precision determination of small energy shifts in Mössbauer spectroscopy, Phys. Rev. B. **30**, 2345 (1984).

37. R.N. Shakhmuratov, F. Vagizov, and O. Kocharovskaya Radiation burst from a single γ-photon field, Phys. Rev. A. **84**, 043820 (2011).

38. Yu. V. Shvyd'ko, S. L. Popov, G. V. Smirnov, Resonant forward nuclear scattering of γ rays after a stepped change in the energy of an excited nuclear state, JEPT Lett. **53**, 231 (1991).

39. Yu. V. Shvyd'ko, S. L. Popov, G. V. Smirnov, Coherent re-emission of γ-quanta in the forward direction after a stepwise change of the energy of nuclear excitation, J. Phys.: Condensed Matter **5**, 1557 (1993).

40. Yu. V. Shvyd'ko, T. Hertrich, U. van Bürck, E. Gerdau, O. Leupold, J. Metge, H. D. Rüter, S. Schwendy, G. V. Smirnov, W. Potzel, and P. Schindelmann, Storage of Nuclear Excitation Energy through Magnetic Switching, Phys. Rev. Lett. **77**, 3232 (1996).

41. R. Röhlsberger, K. Schlage, B. Sahoo, S. Couet, and R. Rüffer, Collective Lamb Shift in Single-Photon Superradiance, Science **328**, 1248 (2010).

42. R. Röhlsberger, H-C. Wille, K. Schlage, and B. Sahoo, Electromagnetically induced transparency with resonant nuclei in a cavity, Nature **482**, 199 (2012).

43. R. Shakhmuratov, F. Vagizov, and O. Kocharovskaya, Single γ-photon revival and radiation burst in a sandwich absorber. Phys. Rev. A **87**, 013807 (2013).

44. K. P. Heeg, H.-C. Wille, K. Schlage, T. Guryeva, D. Schumacher, I. Uschmann, K. S. Schulze, B. Marx, T. Kämpfer, G. G. Paulus, R. Röhlsberger, and J. Evers, Vacuum-Assisted Generation and Control of Atomic Coherences at X-Ray Energies, Phys. Rev. Lett. **111**, 073601 (2013).

45. F. Vagizov, V. Antonov, Y.V. Radeonychev, R.N. Shakhmuratov, and O. Kocharovskaya, Coherent control of the waveforms of recoilless γ-photons, Nature, **508**, 80-83 (2014).

46. R.N. Shakhmuratov, F.G. Vagizov, V.A. Antonov, Y.V. Radeonychev, O. Kocharovskaya, and M. Scully, Transformation of a single-photon field into bunches of pulses, Accepted in Phys. Rev. A.

47. V.A. Antonov, Y.V. Radeonychev, O. Kocharovskaya, γ-ray-pulse formation in a vibrating recoilless resonant absorber, Accepted in Phys.Rev. A.

48. Y.V. Radeonychev, M.D. Tokman, A.G. Litvak, and O. Kocharovskaya, Acoustically induced transparency and generation of multifrequency radiation, Laser Physics, **13**, 1308 (2003).

49. Y.V. Radeonychev, M.D. Tokman, A.G. Litvak, and O. Kocharovskaya, Acoustically induced transparency in optically dense resonance medium, Phys. Rev. Lett. **96**, 093602 (2006).

50. Y.V. Radeonychev, V.A. Polovinkin, and Olga Kocharovskaya, Pulse shaping via modulation of resonant absorption, Laser Physics, **19**, 769 (2009).
51. V.A. Polovinkin, E.V. Radeonychev, Formation of optical pulses by modulating the resonant quantum transition frequency in a spectrally inhomogeneous medium, Quantum Electronics **40**, 115 (2010).
52. Y.V. Radeonychev, V.A. Polovinkin, and Olga Kocharovskaya, Extremely Short Pulses via Stark Modulation of the Atomic Transition Frequencies, Phys. Rev. Lett. **105**, 183902 (2010).
53. Y.V. Radeonychev, V.A. Polovinkin, and O. Kocharovskaya, Extremely short pulses via resonantly induced transparency, Laser Physics **21**, 1243 (2011).
54. V.A. Polovinkin, Y.V. Radeonychev, and O. Kocharovskaya, Few-cycle attosecond pulses via periodic resonance interaction with hydrogen-like atoms, Optics Letters, **36**, 2296 (2011).
55. Y.V. Radeonychev, V.A. Polovinkin, and O. Kocharovskaya, Resonant generation of few-cycle pulses in hydrogenlike atoms, Laser Physics, **22**, 1547 (2012).
56. V.A. Antonov, Y.V. Radeonychev, and O. Kocharovskaya, Formation of a single attosecond pulse via interaction of resonant radiation with a strongly perturbed atomic transition, Phys. Rev. Lett. **110**, 213903 (2013).
57. Y.V. Radeonychev, V.A. Antonov, and O. Kocharovskaya, Resonant formation of few-cycle pulses by hydrogenlike atoms with time-dependent resonance, Laser Physics, **23** 085303 (2013).
58. V. A. Antonov, Y. V. Radeonychev, and Olga Kocharovskaya, Formation of ultrashort pulses via quantum interference between Stark-split atomic transitions in a hydrogenlike medium, Physical Review A, **88**, 053849 (2013).
59. M.J. Berger, J.H. Hubbell, S.M. Seltzer, J. Chang, J.S. Coursey, R. Sukumar, D.S. Zucker, and K. Olsen, XCOM: Photon Cross Sections Database, NIST Standard Reference Database 8 (XGAM), 1998
60. A. Ambrosy and K. Holdik, Piezoelectric PVDF films as ultrasonic transducers, J. Phys. E: Sci. Instrum. **17,** 856 (1984).
61. B.P. Sorokin, G.M. Kvashnin, A.P. Volkov, V.S. Bormashov, V.V. Aksenenkov, M.S. Kuznetsov, G.I. Gordeev, and A.V. Telichko, AlN/single crystalline diamond piezoelectric structure as a high overtone bulk acoustic resonator, Appl. Phys. Lett. **102**, 113507 (2013).
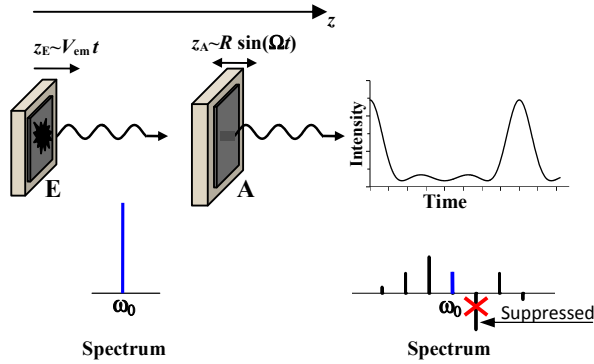
Fig. 1. (Color online) The sketch of the technique (upper part) used in [45] to convert quasi-monochromatic radiation emitted by a Mössbauer radioactive source into a comb of phase-aligned spectral components (lower part) corresponding to periodic sequence of short γ-ray pulses. Radioactive source "E" (a foil with ^{57}Co) emits 14.4keV quasi-monochromatic recoilless radiation with frequency ω_0. A stainless steel foil "A" contains ^{57}Fe nuclei with resonant to ω_0 quantum transition. Vibration of the stainless steel foil leads to harmonic modulation of ω_0 relative to nuclear transition frequency of ^{57}Fe due to the Doppler effect. As a result, the response of ^{57}Fe nuclei constitutes a comb of in-phase spectral components and antiphase components (shifted by π in respect to the in-phase components). In optimal case (see the text) interference of the multifrequency nuclear response with the incident radiation results in suppression of the anti-phase spectral components and formation of the phase-aligned spectrum corresponding to periodic sequence of short γ-ray pulses.
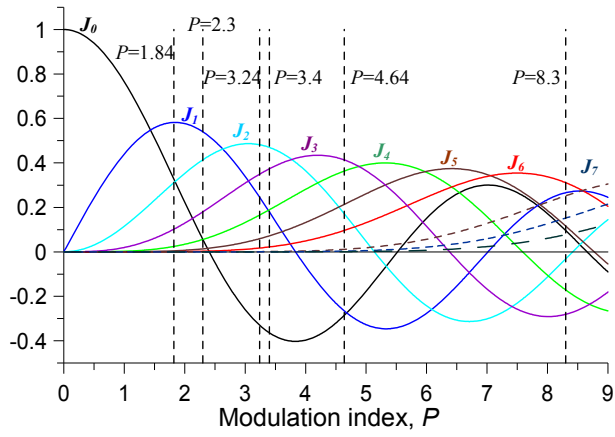
Fig. 2. (Color online) Bessel functions from $J_0(P)$ up to $J_{10}(P)$ versus modulation index, P. The dashed not labeled lines starting up from zero more and more gradually, correspond to $J_8(P)$, $J_9(P)$, and $J_{10}(P)$, respectively. Amplitudes and initial phases of the respective spectral components in (5) are determined by order of the Bessel function, taking into account the relation $J_{-n} = (-1)^n J_n$
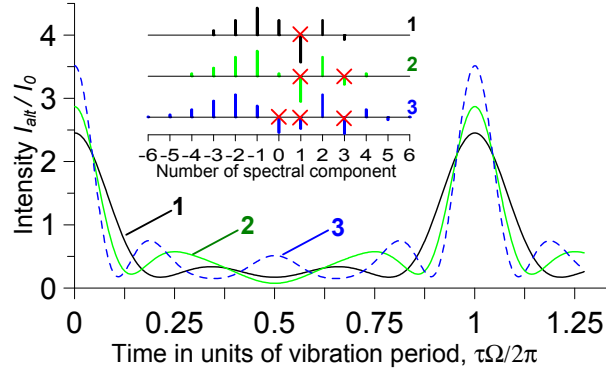
Fig.3. (Color online) Normalized intensity of the transformed γ-radiation, I_{tr}/I_0, produced from the frequency modulated radiation, (3), via deletion of the first component from the spectrum (5) at modulation index P=1.84 (black line #1 and the corresponding spectrum #1 in inset); the first and third spectral components at modulation index P=2.3 (green line #2 and the corresponding spectrum #2 in inset); zero, first and third spectral components at modulation index P=3.24 (blue dashed line #3 and the corresponding spectrum #3 in inset) in one, two, and three ideal resonant absorbers, respectively, with T_A=5. Intensity of the transformed radiation, $I_{tr}/I_0 = I_{del}^{pha}/I_0$, takes into account the photoelectric absorption in ideal ^{57}Fe absorbers. In inset, relative amplitudes and initial phases of spectral components of the field (3), (5) are represented by the vertical bars (in arbitrary units). The in-phase components are above the x-axis while the antiphase components are below the x-axis. The deleted spectral components are marked by red criss-crosses.
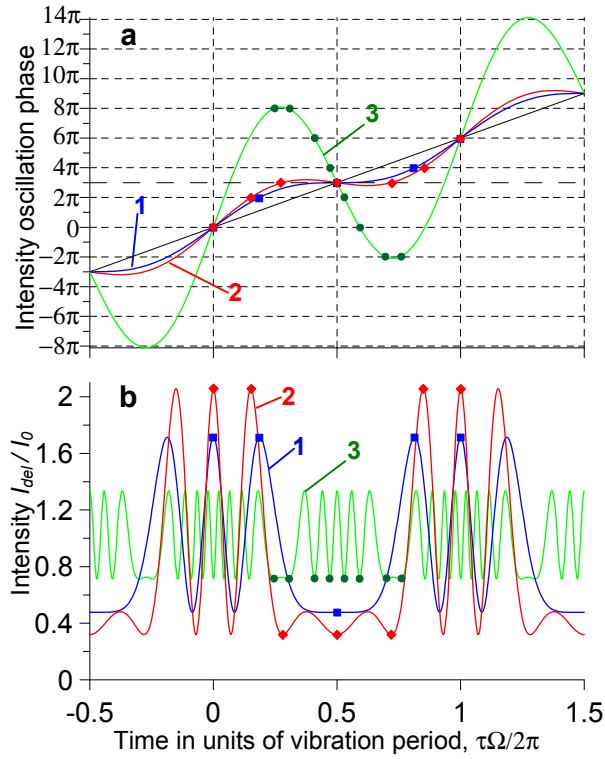
Fig.4. (Color online) **a**: Phase, $\Phi(\tau) = P\sin(\Omega\tau) + a\Omega\tau$, of intensity oscillation, (7), versus time normalized to the vibration period, for the case of the third ($a=3$) deleted spectral component from the spectrum (5) subject to $P=a=3$ (blue line #1), $P=4.2$ (red line #2), $P=20.5$ (green line #3); **b**: the corresponding normalized intensities of γ-radiation, I_{del}^{pha}/I_0.
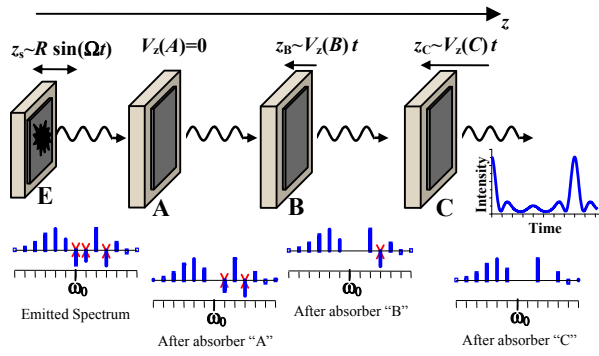
Fig.5. (Color online) The sketch of the technique (upper part) to convert frequency modulated radiation emitted by vibrating Mössbauer radioactive source into a periodic sequence of short γ-ray pulses by three sequentially placed resonant absorbers in the case of Fig.3 (blue dashed line #3). Vibrating radioactive source "E" (a foil with ^{57}Co) emits a comb of in-phase spectral components and antiphase components (shifted by π in respect to the in-phase components). Anti-phase components that should be removed are marked by red criss-crosses.
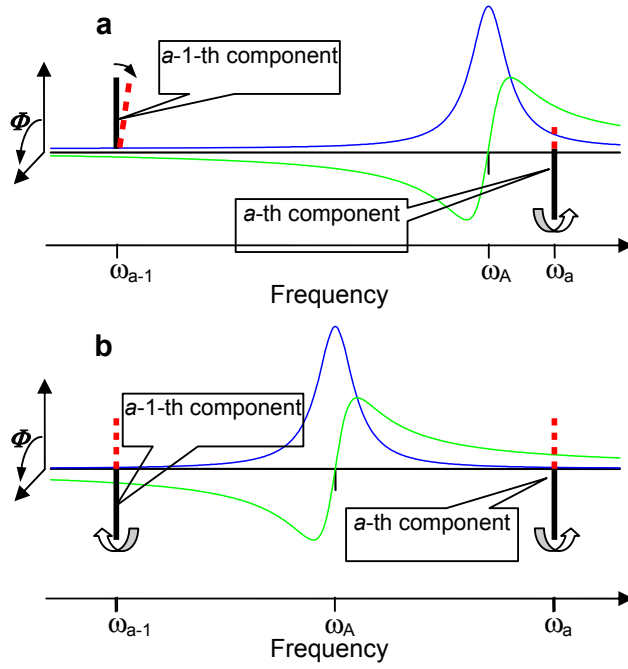
a

a-1-th component

a-th component

Φ

ω_{a-1} ω_A ω_a

Frequency

b

a-1-th component

a-th component

Φ

ω_{a-1} ω_A ω_a

Frequency

Fig.6. (Color online) Relative amplitudes (vertical bars in arbitrary units) and initial phases, Φ, of the *a*-th and *a*-1-th spectral components of the frequency modulated field (3), (5) before (black bars) and after (red dashed bars) alteration in a resonant absorber. The in-phase components are above the x-axis while the antiphase components are below the x-axis. Green and blue lines represent spectral profiles of the resonant dispersion and absorption, respectively, of an absorber. **a**: Inversion of initial phase of the *a*-th antiphase spectral component via the resonant dispersion of an absorber is accompanied by its attenuation due to the resonant absorption. The nearest *a*-1-th spectral component acquires a phase shift due to the resonant dispersion. The absorber has Mössbauer thickness $T_A=20.9$, its spectral line with halfwidth γ_A is detuned from the frequency of the *a*-th spectral component by $\delta_a=3\gamma_A$, the absorber vibrates with frequency $\Omega=20\gamma_A$. **b**: Simultaneous inversion of initial phases of the *a*-th and *a*−1-th antiphase spectral components via the resonant dispersion of absorber with taking into account their attenuation due to the resonant absorption. The Mössbauer thickness of absorber is $T_A=63.5$.
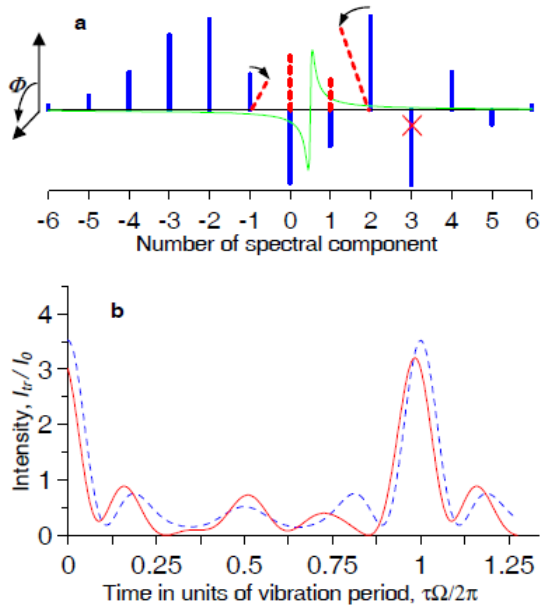
Fig.7. (Color online) **a**: Relative amplitudes (vertical bars in arbitrary units) and initial phases, Φ, of spectral components of the frequency modulated field (3), (5) at optimal modulation index $P=3.4$ and modulation frequency $\Omega=20\gamma_A$ before (blue bars) and after (red dashed bars) alteration in two resonant absorbers (unchanged components are the same blue bars). The in-phase components are above the x-axis while the antiphase components are below the x-axis. One absorber with $T_A=63.5$ inverts initial phases of zero and the first components via its resonant dispersion (green curve) and reduces their amplitudes because of the resonant absorption as well as changes initial phases of the adjacent components by $\pm\pi/3$ and slightly attenuates them. Another absorber with $T_A=5$ deletes the third component (marked by criss-cross). **b:** The normalized intensity of the transformed field, $I_{tr}/I_0 = I_{inv}^{pha}/I_0$, red curve, in comparison with intensity of the field formed in three resonant absorbers deleting all three spectral components at optimal modulation index $P=3.24$, $I_{tr}/I_0 = I_{del}^{pha}/I_0$ (blue dashed line which is the same as blue dashed line #3 in Fig.2). Both curves take into account non-resonant photoelectric absorption of the field as a whole for the case of ideal [57]Fe absorbers.
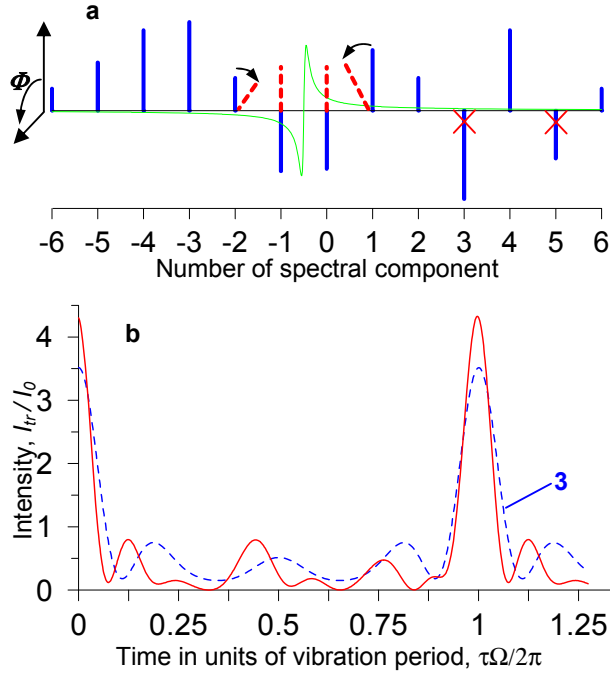
Fig.8. (Color online) **a**: Relative amplitudes (vertical bars in arbitrary units) and initial phases, Φ, of spectral components of the frequency modulated field (3), (5) at optimal modulation index P=4.7 and modulation frequency Ω=20γ_A before (blue bars) and after (red dashed bars) alteration in three resonant absorbers (unchanged components are the same blue bars). The in-phase components are above the x-axis while the antiphase components are below the x-axis. One absorber with T_A=63.5 inverts initial phases of the minus first and zero components via its resonant dispersion (green curve) and reduces their amplitudes because of the resonant absorption as well as changes initial phases of the adjacent components by $\pm\pi/3$ and slightly attenuates them. Two other absorbers with T_A=5 delete the third and fifth components (marked by criss-crosses). **b:** The normalized intensity of the transformed field, $I_{tr}/I_0 = I_{inv}^{pha}/I_0$, red curve, in comparison with intensity of the field formed in three resonant absorbers deleting three spectral components at optimal modulation index P=3.24, $I_{tr}/I_0 = I_{del}^{pha}/I_0$ (blue dashed line #3 which is the same as blue dashed line #3 in Fig.2). Both curves take into account non-resonant photoelectric absorption of the field as a whole for the case of ideal ^{57}Fe absorbers. Peak intensity of red pulses is 1.23 of peak intensity of blue pulses. In the case of stainless steel absorbers fully enriched by ^{57}Fe, this ratio is 1.13. The red pulse duration is about 0.08T, corresponding to 8 ns in the case where vibration frequency is 1/T=10 MHz.
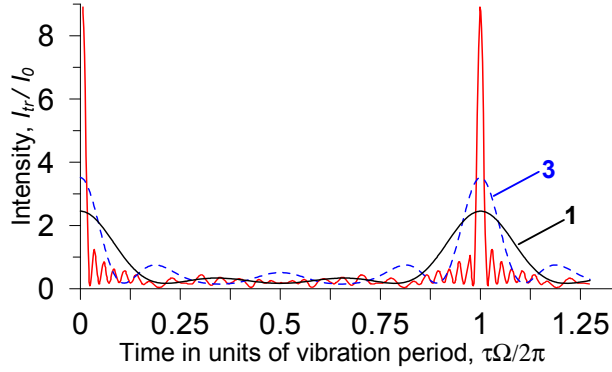
Fig.9. (Color online) The normalized intensity of the transformed field, $I_{tr}/I_0 = I_{del}^{pha}/I_0$, produced by deletion of 22 antiphase components in 22 resonant absorbers with $T_A=5$ from the spectrum of the frequency modulated field (3), (5) consisting of 52 components at optimal modulation index $P=20.1$ and modulation frequency $\Omega=20\gamma_A$ (red curve) in comparison with intensity of the field produced by deletion of three spectral components at optimal modulation index $P=3.24$ (blue dashed line #3 which is the same as blue dashed line #3 in Fig.2) and by deletion of a single spectral component at optimal modulation index $P=1.84$ (black line #1 which is the same as black line #1 in Fig.2). All the curves take into account non-resonant photoelectric absorption of the field as a whole for the case of ideal ^{57}Fe absorbers. Peak intensity of red pulses is $8.96I_0$. In the case of stainless steel absorbers fully enriched by ^{57}Fe, peak intensity of red pulses is $7.6I_0$. The red pulse duration is about $0.02T$, corresponding to 1 ns in the case where vibration frequency is $1/T=20$ MHz.